PERFORMANCE IMPROVEMENT OF A LINEAR ENCODER BY MULTIRATE SAMPLING OBSERVER

Lilit Kovudhikulrungsri
Department Electrical Engineering
The University of Tokyo
7-3-1 Hongo, Bunkyo-ku, Tokyo 113-8656, JAPAN
Tel: +81 3 5841 6791 Fax: +81 3 5800 5988
Email: lilit@koseki.t.u-tokyo.ac.jp

Takafumi Koseki
Department of Information and Communication
The University of Tokyo
7-3-1 Hongo, Bunkyo-ku, Tokyo 113-8656, JAPAN
Tel: +81 3 5841 6791 Fax: +81 3 5800 5988
Email: koseki@koseki.t.u-tokyo.ac.jp

***Abstract*—This paper describes an effective way to improve the performance of a linear encoder by introducing an estimation technique called multirate sampling observer. The authors analyses the observer by using multirate sampling theory and verifies its effectiveness by various Simulations.**

***Key words*—Linear encoder, multirate sampling observer , position and speed estimation.**

1. INTRODUCTION

Linear encoders are simple sensing devices for linear motion. The resolutions of these encoders depend on the linear scales and the optical sensors. Recent developments in sensing techniques allow us to obtain high precision and accuracy. The costs of high-precision sensors are, however, very expensive. Using less-precision linear encoders is a more economical solution but this causes the problem in control, especially at low speed.

Fig. 1 illustrates the condition at low speed. The arrows stand for pulses, which are the outputs of an encoder. The period between two consecutive pulses, T_1, is longer than the control period, T_2. As a result, we cannot control the system precisely.

To solve this problem, we apply an estimation scheme called "multirate sampling observer", which is a specific discrete-time observer to estimate the speed and position between two consecutive pulses. The effectiveness of the observer is verified through various simulations.

2. MULTIRATE SAMPLING OBSERVER

2.1. Derivation

Derivation of the multirate sampling observer is based on the timing diagram in Fig. 1, where T_1 is the interval between the pulses, T_2 is the control of sampling period, m is the number of the pulse and n is the number of the sampling instant after the pulse is detected. The block diagram of the observer is shown in Fig. 2. The observer is derived from a speed observer in discrete-time domain with disturbance dynamics consideration.

$$\hat{\mathbf{x}}[n+1] = (\mathbf{A_2} - \mathbf{L_2 C_2})\hat{\mathbf{x}}[n] + \mathbf{B_2}u[n] + \mathbf{C_2}y[n] \qquad (1)$$

where $\hat{\mathbf{x}} = \begin{bmatrix}\hat{r} & \hat{v} & \hat{F}_L\end{bmatrix}^T$, $u = F_m$ and $y = x$. r, v, F_L and F_m represent position, speed, disturbance force and driving force, e.g. from a linear motor , respectively. $\mathbf{L_2}$ is the observer gain matrix. Note that the input u and the output y in this case are scalar quantities, but generally they can be vectors based on the state space description. The subscript 2 indicates that the constant DSP clock T_2 is used as the sampling time of the system and the symbol ^ indicates the estimated value. Matrices $\mathbf{A_2}$, $\mathbf{B_2}$ and $\mathbf{C_2}$ are derived from their continuous time domain matrices with disturbance consideration $\mathbf{A}$, $\mathbf{B}$ and $\mathbf{C}$, respectively. The components of these matrices are described as follow

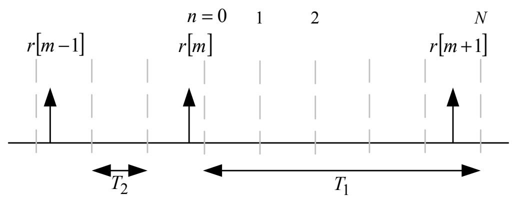

Figure. 1 Timing diagram

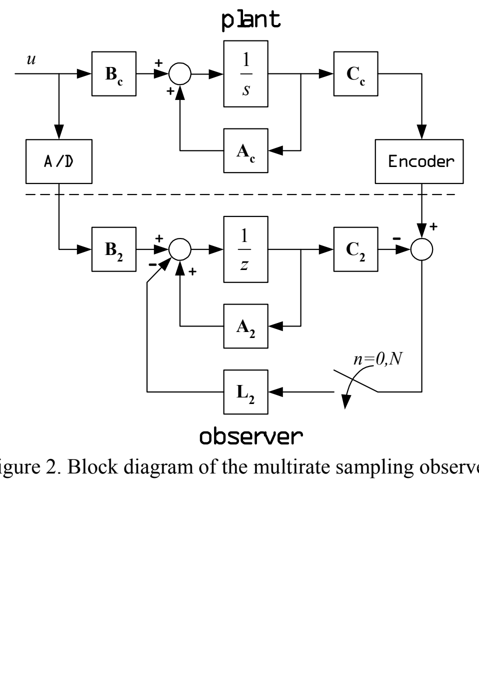

Figure 2. Block diagram of the multirate sampling observer

$$\mathbf{A}=\begin{bmatrix}0 & 1 & 0\\ 0 & 0 & 1/M\\ 0 & 0 & 0\end{bmatrix},\mathbf{B}=\begin{bmatrix}0\\ 1/M\\ 0\end{bmatrix},\mathbf{C}=\begin{bmatrix}1 & 0 & 0\end{bmatrix}, \tag{2}$$

where M is the mass of the moving part. Hence, the plant in this case is only the mechanical dynamics of the moving part, which can be described as follow

$$\mathbf{x}=\mathbf{A_c}\mathbf{x}+\mathbf{B_c}u, y=\mathbf{C_c}\mathbf{x} \tag{3}$$

where $\mathbf{A_c}=\begin{bmatrix}0 & 1\\ 0 & 0\end{bmatrix}$, $\mathbf{B_c}=\begin{bmatrix}0\\ 1/M\end{bmatrix}$, $\mathbf{C_c}=\begin{bmatrix}1 & 0\end{bmatrix}$, $\mathbf{x}=\begin{bmatrix}r\\ v\end{bmatrix}$.

Fig. 3 shows a diagram of discrete time signals. Thick arrows represent actual values and thin arrows stand for estimated values. We define periods between the detected pulses as sampling frames. Hence, the interval of each sampling frame has the period of T_1. From the diagram, the actual output y or the shaft angle can be obtained only when an encoder pulse is detected. At this moment, the error of estimation is corrected. On the other hand, when pulses are not detected, the observer principally works as a simulator, calculating the state variables based on the plant model. This condition is achieved by using the estimated shaft angle when the detected pulses are not available as illustrated in the diagram. This method is practical in both simulations and experiments since it can be programmed easily. This leads to the assumption that

$$y=\begin{cases}y, & n=0,N; N=T1/T2\\ \hat{y}, & \text{otherwise}\end{cases}, \tag{4}$$

where n is the sampling index in each sampling frame, N is the last sampling instant in each frame. Hence, the observer equations can be expressed as follow

$$n=0,N\ ;\ \hat{\mathbf{x}}_{n+1}=\mathbf{A_2}\hat{\mathbf{x}}_n+\mathbf{B_2}u_n+\mathbf{L_2}\left(y_n-\hat{y}_n\right), \tag{5}$$

$$n\neq 0,N\ ;\qquad \hat{\mathbf{x}}_{n+1}=\mathbf{A_2}\hat{\mathbf{x}}_n+\mathbf{B_2}u_n. \tag{6}$$

Due to this fact, the last sampling instant in each sampling frame decides the dynamics of the next sampling frame. Dynamics of each frame can be expressed by

$$\begin{aligned}\hat{\mathbf{x}}_\mathbf{n}&=\mathbf{A_2}^{n-1}\left(\mathbf{A_2}-\mathbf{L_2C_2}\right)\hat{\mathbf{x}}_0+\mathbf{A_2}^{n-1}\mathbf{B_2}u_0+\\ &\mathbf{A_2}^{n-2}\mathbf{B_2}u_1+\cdots+\mathbf{A_2}^{0}\mathbf{B_2}u_{n-1}+\mathbf{A_2}^{n-1}\mathbf{L_2}y_0\end{aligned} \tag{7}$$

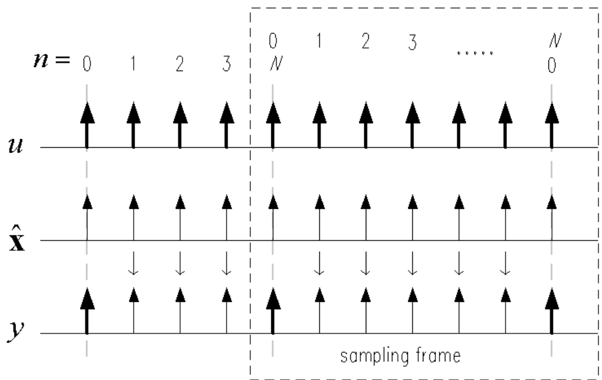

Figure 3. Discrete-time signals

2.2. Pole Placement

To place the observer poles, let's rearrange (7) to obtain

$$\hat{\mathbf{X}}[m+1]=\overline{\mathbf{A}}\hat{\mathbf{X}}[m]+\overline{\mathbf{B}}\mathbf{U}[m]+\overline{\mathbf{L}}y_0[m], \tag{8}$$

where $\overline{\mathbf{A}}=\begin{bmatrix}\mathbf{0} & \mathbf{0} & \cdots & \left(\mathbf{A_2}-\mathbf{L_2C_2}\right)\\ \mathbf{0} & \mathbf{0} & \cdots & \mathbf{A_2}\left(\mathbf{A_2}-\mathbf{L_2C_2}\right)\\ \vdots & \vdots & \ddots & \vdots\\ \mathbf{0} & \mathbf{0} & \cdots & \mathbf{A_2}^{N-1}\left(\mathbf{A_2}-\mathbf{L_2C_2}\right)\end{bmatrix}$,

$\overline{\mathbf{B}}=\begin{bmatrix}\mathbf{B_2} & \mathbf{0} & \cdots & \mathbf{0}\\ \mathbf{A_2B_2} & \mathbf{B} & \cdots & \mathbf{0}\\ \vdots & \vdots & \ddots & \vdots\\ \mathbf{A_2}^{N-1}\mathbf{B_2} & \mathbf{A_2}^{N-2}\mathbf{B_2} & \cdots & \mathbf{B_2}\end{bmatrix}$, $\overline{\mathbf{L}}=\begin{bmatrix}\mathbf{L_2}\\ \mathbf{A_2L_2}\\ \vdots\\ \mathbf{A_2}^{N-1}\mathbf{L_2}\end{bmatrix}$,

$\hat{\mathbf{X}}[m]=\begin{bmatrix}\hat{\mathbf{x}}[m,1]\\ \hat{\mathbf{x}}[m,2]\\ \vdots\\ \hat{\mathbf{x}}[m.N]\end{bmatrix}$ and $\mathbf{U}[m]=\begin{bmatrix}u[m,0]\\ u[m,1]\\ \vdots\\ u[m,N-1]\end{bmatrix}$.

Poles of the observer are obtained by solving the following equation

$$\mathrm{eig}(\overline{\mathbf{A}})=\mathrm{eig}\left(\mathbf{A_2}^{N-1}\left(\mathbf{A_2}-\mathbf{L_2C_2}\right)\right)=\left|z_2\mathbf{I}-\overline{\mathbf{A}}\right|=0, \tag{9}$$

where z_2 is the Z-transform variable due to the constant sampling time T_2, *i.e.* z_2-domain.

$$z_2=\exp(T_2s). \tag{10}$$

Solving (9), we discover the fact that there are $3N$ poles on z_2-plane. Among these, there are only 3 poles that do not locate at the origin. Hence, we can place these 3 poles to adjust the dynamics of the observer.

2.3. Observer gains, pole location and their relationship when sampled by the variable sampling time T_1 and the constant sampling time T_2

T_1 is defined as the period between two consecutive pulses, so it always varies dependently on speed. When dealing with a variable-sampling-time system, a controller and an observer are conventionally designed at a nominal speed or nominal operating point by fixing the poles of z-plane. This method works effectively at nominal speed but the response of the system deteriorates at relatively different speed. Observer equation is described by

$$\hat{\mathbf{x}}[m+1]=\mathbf{A_1}\hat{\mathbf{x}}[m]+\mathbf{B_1}u[m]+\mathbf{L_1}\left(y[m]-\hat{y}[m]\right). \tag{11}$$

Note that subscript 1 indicates that T_1 is used as a sampling time, i.e. z_1-domain. To find the relationship between both domains, let's assume that the input signals in each sampling frame in z_2-domain are constant. (7) can be rearranged as follow

$$\hat{\mathbf{x}}[m+1]=\mathbf{A_1}\hat{\mathbf{x}}[m]+\mathbf{B_1}u[m]+\mathbf{A_2}^{N-1}\mathbf{L_2}\left(y[m]-\hat{y}[m]\right). \tag{12}$$

Comparing (11) and (12) leads to the following relation

$$\mathbf{L_1} = \mathbf{A_2}^{N-1}\mathbf{L_2} \text{ or } \mathbf{L_2} = \left(\mathbf{A_2}^{N-1}\right)^{-1}\mathbf{L_1} . \qquad (13)$$

Substituting the value of $\mathbf{L_2}$ in (9) and using the fact that $\mathbf{C_1}$ equals to $\mathbf{C_2}$, we obtain

$$\mathrm{eig}(\mathbf{A_1} - \mathbf{L_1}\mathbf{C_1}) = \left| z_1\mathbf{I} - (\mathbf{A_1} - \mathbf{L_1}\mathbf{C_1}) \right| = 0 \qquad (14)$$

Hence, the poles on z_2-plane that are not located at the origin are identical to the poles on z_1-plane.

2.4. Gain tuning procedures

The gain of the multirate sampling observer can be simply tuned by consideration of the relationship of the sampling time T_1 and T_2 or based on (13) and (14) derived in the previous section. The gain tuning procedure is concluded as follow

1.) Placing the pole on z_1-plane and calculating the observer gain in z_1-domain, $\mathbf{L_1}$, by using (13)

2.) Using the relationship in (14) to calculate the observer gain in z_2-domain $\mathbf{L_2}$.

The observer gain $\mathbf{L_2}$ is variable according to the number of the intersampling or the ratio of T_1 to T_2, N. In real application, we can easily apply this gain tuning by off-line calculation and using a look-up table. The calculated observer gains are shown in Fig. 4

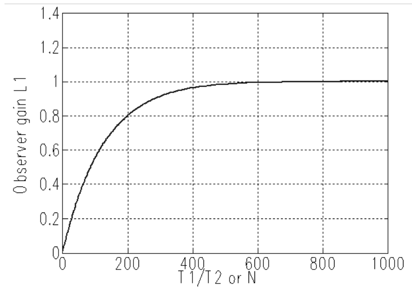

(a) Observer gain L1

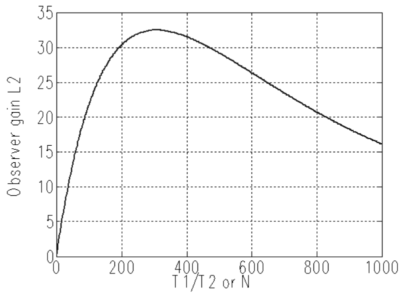

(b) Observer gain L2

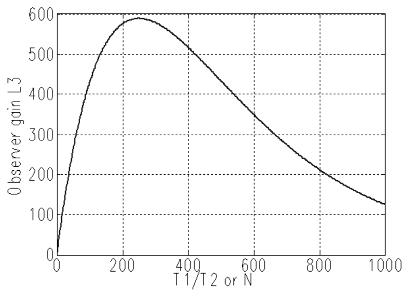

(c) Observer gain L3

Figure 4. Observer gains

3. SIMULATION RESULTS

In order to verify the performance of the multirate sampling observer, we apply the observer to a simple one-mass system driven by a linear actuator. The plant model in state space description is shown in (3). Note that the matrix $\mathbf{C_c}$ can be changed to [0 1] for speed control.

The block diagram for verification is shown in Fig. 5. It is a simple state feedback with integral term. We use a low-cost linear scale with the resolution of 1 mm and the mass of the moving part is 1 kg.

Fig. 6 shows the position response against a step trajectory. The command is set to 10.5 mm. Note that the resolution of the encoder is 1 mm, so the command is between two consecutive marks on the linear scale. Fig. 6(a) and (b) show the responses when the encoder's information is directly used and when the multirate sampling observer is applied, respectively. Their larger views are shown in Fig. 6(c) and (d), respectively. It is obviously seen that the observer can estimated an accurate value so the response of the plant precisely tracks the command. On the other hand, the response when the encoder's information is directly used oscillates because of the limitation of the resolution.

Another merit of using the multirate sampling observer is that it can estimate the disturbance. The estimated disturbance is then used a feedforward compensation to improve the robustness of the system. According to the result in Fig. 6(a) and (b), a step disturbance force of 0.1 N is applied at the fifth second. This causes a big deviation in case of the conventional method in Fig. 6(a). Oppositely, the response of the system with the multirate sampling observer is much more robust to the disturbance as shown in Fig. 6(b)

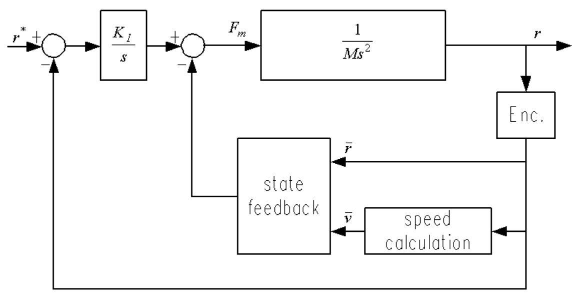

(a) Conventional encoder signal feedback

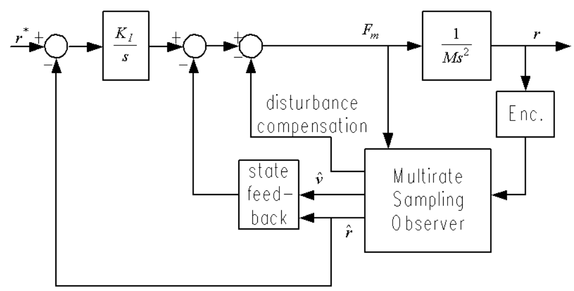

(b) The proposed control system with multirate sampling observer

Figure 5. Block diagram for verification of the performance of the multirate sampling observer

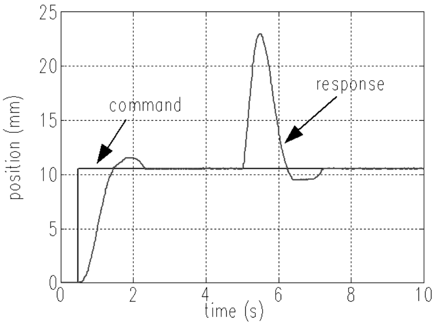

(a) Response when the encoder's information is directly used

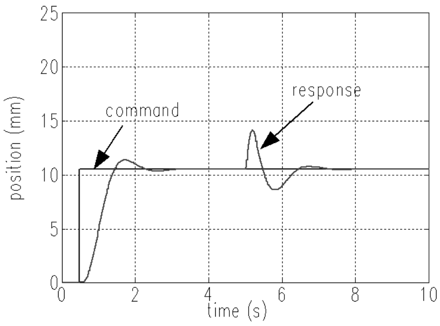

(b) Response when the multirate sampling observer is applied

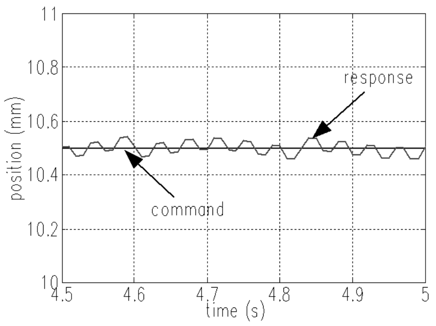

(c) A larger view of (a)

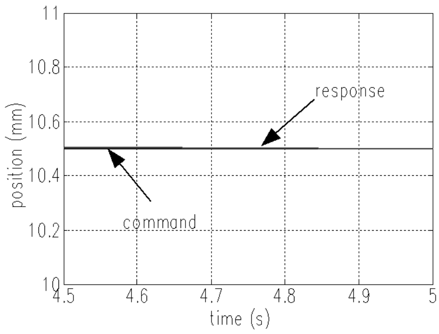

(d) A larger view of (b)

Figure 6 Simulation results based on a step command

Fig. 7 shows responses when a constant speed command of 1 m/s is applied. At the fifth second, a step disturbance of 10 N is injected. The response in Fig. 7(a), in which the encoder's information is directly used, is noisy. The multirate sampling observer can estimate the speed, which has low noise and the estimated disturbance can be used for feedforward compensation, so the response is improved as shown in Fig. 7(b).

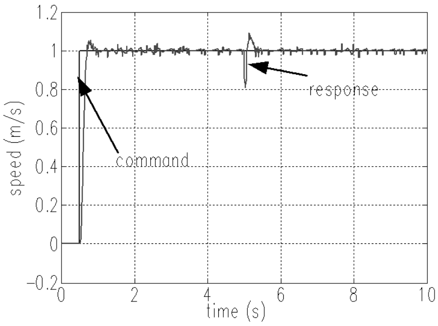

(a) Response when the encoder's information is directly used

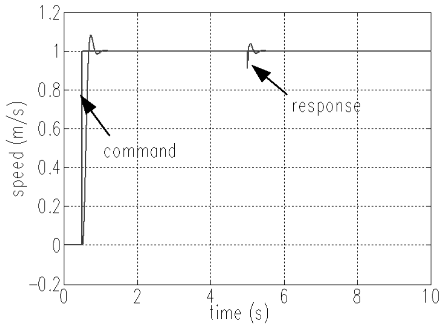

(b) Response when the multirate sampling observer is applied

Figure 7. Simulation results based on a speed command

4. CONCLUSIONS

This paper has described an effective way to improve the performance of a linear encoder by introducing an estimating technique called "multirate sampling observer". The multirate sampling observer is a specific discrete-time observer that can estimate precise speed, position and other state variables between two consecutive encoder pulses. We have also proposed a pole placement method, which results in variable gains. This method stabilized the operation even at stand still condition. The observer can also estimate the disturbance, which is used to improve the robustness of the system by feedforward compensation. Various simulation results have shown that the multirate sampling observer can improve the performance of a linear encoder.

REFERENCES

[1] Y. Hori, "Robust Motion Control Based on a Two-Degrees of-Freedom Servosystem", Advanced Robotics, vol.7, No.6, pp.525-546, 1993.
[2] M. Araki, K. Yamamoto, "Multivariable Multirate Sampled-Data System: State-Space Description, Transfer Characteristics and Nyquist Criterion", IEEE Trans. Automatic Control, vol. AC-31, pp.145-154, 1986..
[3] L. Kovudhikulrungsri, T. Koseki, "Precise Torque and Speed Control In Pure Electric Braking Operation of AC Traction in Low Speed Range", International Workshop on Advance Motion Control, pp.142-147, Maribor, Slovenia, Jul., 2002
[4] L. Kovudhikulrungsri, T.Koseki, "Improvement of Performance and Stability of a Drive System with a Low-Resolution Position Sensor by Multirate Sampling Observer", Proc. The 2003 Japan Industry Application Society Conference, Tokyo, Japan, Aug., 2003